Evaluation of In Situ Thermomechanical Stress-Strain in Power Modules using Laser Displacement Sensors

Jørgensen, Asger Bjørn; Munk-Nielsen, Stig; Uhrenfeldt, Christian

Published in:
I E E E Transactions on Power Electronics

DOI (link to publication from Publisher):
10.1109/TPEL.2021.3054336

Publication date:
2021

Document Version
Accepted author manuscript, peer reviewed version

Evaluation of In Situ Thermomechanical Stress-Strain in Power Modules using Laser Displacement Sensors

Asger Bjørn Jørgensen, Stig Munk-Nielsen and Christian Uhrenfeldt

***Abstract*—Digital design has been successfully employed in development of new compact wide bandgap power modules, achieving unprecedented switching speeds while maintaining low thermal resistance. Owing to the achieved performance, the next step in the field is ensuring that proposed designs are mechanically robust and reliable. The new power module structures lack the long history of experimental experience as is the case with conventional silicon power modules. To limit the number of physical prototypes that needs to be built and to speed up development time, having a verified simulation model of the thermomechanical behavior is of great value to designers. In this paper a finite element simulation of the thermomechanical induced stress and strain is presented of an integrated GaN full-bridge switching cell. The simulated strain of the power module is verified by an experimental test. During the test, one of the semiconductor devices of the module is subjected to a power loss. A laser displacement sensor is used to measure the in-situ deflection of the ceramic substrate caused by the temperature increase. The experimental results confirm the ability of the simulation model to accurately predict the deflection within an error of only 7.3 %.**

***Index Terms*—Finite element methods, Laser measurements, Semiconductor device packaging, Failure analysis.**

I. Introduction

NEW power module packages are being proposed, to better utilize the fast switching potential offered by wide bandgap (WBG) power semiconductors. To achieve clean switching waveforms, several research teams are proposing new integration methods and switching cell concepts to reduce the commutation loop inductance [1]–[3]. During design of these new concepts, finite element methods (FEM) simulations are utilized to solve for the electrical parasitics [4]–[6]. Several design iterations are evaluated until a low inductive packaging is achieved and results in clean switching. Similarly, the thermal performance of the proposed power module structures are being assessed using FEM tools [1], [7], [8]. Such a digital design approach is utilized to minimize the required number of prototypes that have to be built physically, and development time of high performance designs is reduced by a rapid assessment digitally in a simulation environment [9]. In summary, the methodology in terms of evaluating the electro-thermal design is already well-established for these integrated WBG packages. As a next step in the digital design process of integrated power modules, the purpose of this paper is to study the thermomechanical induced stress/strains in an integrated WBG power module.

During operation of the power module, the semiconductor dies dissipate heat due to losses. The power dissipation is periodic in nature, typically related to a grid frequency or rotating speed of a drive. Owing to the periodic power, the temperature throughout the module is changing over time. The various materials in the power module have different coefficients of thermal expansion (CTE) and because they are joined and not free to move, they experience an internal build up in mechanical stress. Depending on the stress-strain relationship of each material, they will expand differently which causes geometrical changes such as warpage or bending [10]. Over time the millions of cycles of stress-strain wears out the integrity of materials and interconnections, which eventually leads to failure of the module [11].

Conventional power module structures has several decades of knowledge to rely on, including: failure-mode analysis, lifetime testing and millions of hours of field operation [12]–[17]. The data available is extensive and builds a strong foundation for engineers to design a power module with high reliability. The opposite is the case for the new integrated and compact WBG power module packages, as they have not yet stood the test of time. Building a strong statistical foundation requires vast amount of resources both in terms of materials used in building enough prototypes to test and time required to cycle the prototypes until failure [18]. Alternatively, the problems related to thermomechanical induced stress are evaluated digitally using FEM software. Predicting the location and amount of thermomechanical stress in the module is important to aid in the improvement of the reliability of future power modules designs [19]–[21]. Setting up a FEM model of a power module often requires complex 3D modelling, knowledge of mixed boundary conditions and a library of material properties, which all can be linked to some degree of uncertainty. To have confidence in the simulated thermomechanical induced stress-strains, it is important to have a step of experimental verification of the FEM model.

Within the topic of power module packaging, the warpage of power module substrates, printed circuit boards and baseplates is a commonly studied thermomechanical effect. Typically, the curvature of the entire surfaces are scanned using methods such as photo processing of surfaces illuminated by Moire patterns [22], [23], gate timing of scanning acoustic microscopes [24] or using a laser deflection sensor to scan parallel lines along the object [25], [26]. These methods are usually

A.B. Jørgensen, S. Munk-Nielsen and C. Uhrenfeldt are with the Department of Energy Technology, Aalborg University, Aalborg 9220, Denmark (e-mail: abj@et.aau.dk, smn@et.aau.dk, chu@et.aau.dk).

used to measure the warpage caused by: large temperature swings during soldering [25], temperature cycling for wear out testing [27] or mechanical assemblies such as molding [28]. The benefit of these methods is that they map the curvature of the entire surface, and thus provide a detailed mapping of the deflection at several points of the investigated surface. The drawback of the mentioned methods is that they require the entire surface to be exposed for it to be scanned. The power module must be removed from its application to be investigated. Thus, the method can be regarded as "offline", because the module is removed from its normal operation to evaluate its warpage. To predict failure mechanisms due to wear out of the power module, it is the thermomechanical stress-strain within the power module during normal operation which is of interest.

In this paper, the purpose is to evaluate the warpage during active heat up of an integrated GaN power module, due to the power losses in one of its semiconductor devices. The measurements are done while the module is operated in its intended application, thus making this an "in situ" evaluation of the stress. The in situ deflection measurement method is proposed in Section II. A 3D FEM simulation model of the stress/strain in an integrated power module based on GaN enhancement high electron mobility transistors (eHEMT) is presented in Section III. In Section IV the experimental results are compared to the 3D FEM simulation model. This is used to validate whether the material parameters, boundary conditions and loads are correctly assigned in the FEM software. Having a validated thermomechanical stress/strain model of the power module is a valuable tool to help power module designers to improve mechanical robustness early in future iterations of the module design. In Section V the validated simulation model is used to discuss the deflection due to active and passive thermal cycling. The paper is concluded in Section VI.

II. Methodology

The integrated GaN eHEMT power module structure used for this study is shown in Fig. 1. A 3D model of the module is assembled i.e. combining the GaN eHEMT devices, printed circuit board (PCB) and direct bonded copper (DBC) substrate. In a previous paper [7], a thermal simulation of the full 3D model of the power module was presented and verified by an experimental test. Thus, this verified thermal distribution from the FEM simulation model is used as the precursor in this paper, for determining the thermomechanical induced stress/strains of the developed module.

The test setup to verify the thermomechanical induced strain is depicted in Fig. 2. A DC current is conducted through one of the semiconductor devices of the module, which due to the on-resistance of the device results in a power loss, P_{loss}. The power loss is conducted through the different layers of the module assembly and absorbed by the heat sink. Due to the thermal resistance of the materials, a temperature difference develops across each layer. The temperature distribution and differences in CTE, causes unequal expansion of materials and results in warpage of the DBC, as indicated in Fig. 2. It is the deflection, δ, measured at the center point of the power

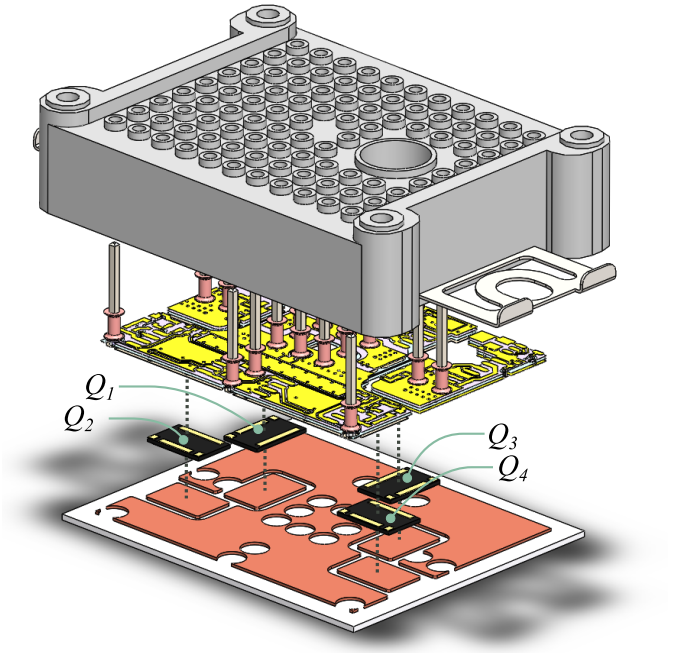

Fig. 1. 3D model of the integrated power module structure with Q_1 ... Q_4 being GaN eHEMT devices from GaN Systems.

module, which is the quantity used for comparison between the simulation and experiment in this paper.

To evaluate the in situ warpage the module should remain mounted to the heat sink as in its intended final application. To experimentally evaluate the deflection of the power module DBC, the use of a laser displacement sensor is proposed. The laser displacement measures the distance to a single point by emitting a light beam. The light beam is reflected, and depending on the distance to the object the light will be registered at different cells of the receiver, as shown in Fig. 2. In [26] the method was used to scan the entire surface of a module through several parallel slits and thus map its curvature over the entire baseplate. However, in this paper only a single hole of small diameter is drilled through the heat sink, placed at the center of the DBC. The purpose of this is to minimize the change in the thermal system as compared to its final application. Because the test only measures the deflection of the power module in a single location, the test will be run at several operating points to ensure that the simulation model is valid within a range.

III. Finite Element Simulation Model

The following section describes how the power module is modelled in 3D, as shown in Fig. 1, and how the simulation has been configured, including details such as: materials, boundary conditions and inputs. The objective is to simulate the thermomechanical stress and strain of the power module, and evaluate deflection of the DBC at the center point to be able to compare it with the experimental results in Section IV.

A simulation framework of different software packages, as proposed in [9], is used to build up the 3D model as shown in Fig. 1. Solidworks is used to design the 3D model of the

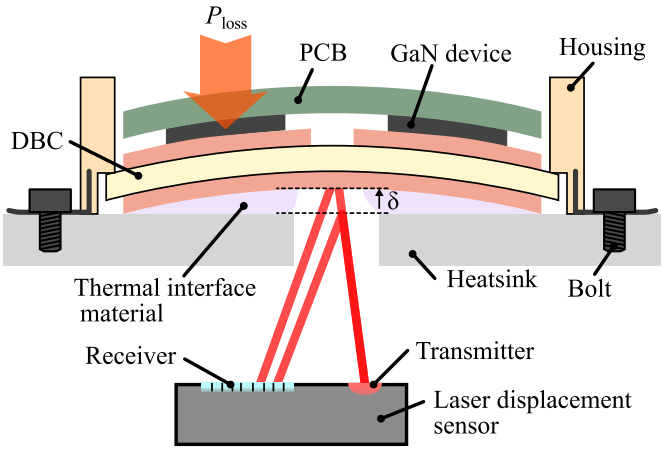

Fig. 2. Principal diagram of the deflection measurement in a power module mounted to a heatsink using laser displacement sensor.

power module excluding the PCB. The PCB is designed in the layout editor PADS, which works with 2D information in different layers. The 2D information is saved in an ODB++ file format and imported to ANSYS Siwave, which translates the 2D layers and the board layer thickness specifications into a 3D CAD file. The 3D model of the PCB is imported into the Solidworks to assemble with the other parts, and the full model of the integrated power module is imported to COMSOL Multiphysics, as shown in Fig. 3. A relatively fine mesh is used to include geometry of the vias in the PCB board, as they significantly influence to the heat distribution between devices in the module [7].

The amount of strain of the power module depends on CTE, Young's modulus and Poisson's ratio of the materials, and the temperature distribution throughout the module, which in itself is dependent on the thermal conductivity. The DBC consists of copper on either side of an aluminium oxide (Al_2O_3) ceramic. The PCB is assigned as copper for its conductive layers and FR4 for the surrounding dielectric. Used material properties are listed in Table I. The GaN devices are modelled as having infinite thermal conductivity and are uniformly heated. By this approach each device block represents the junction temperature, which allows the use of thermal resistances from the datasheet. The thermal resistances of the device are achieved by assigning resistive layers on the terminal interconnections, ensuring a thermal resistance of 0.5 $\frac{K}{W}$ from junction to the heat pad and 5 $\frac{K}{W}$ from junction to the electrical contacts [29].

TABLE I
MATERIAL PROPERTIES USED IN THE SIMULATION MODEL [30]–[32]

Material property	**Cu**	**FR4**	**Al_2O_3**
Thermal conductivity $\left[\frac{\mathrm{W}}{\mathrm{m\cdot K}}\right]$	400	0.3	24
CTE $\left[\frac{1}{\mathrm{K}}\right]$	$17{\cdot}10^{-6}$	$18{\cdot}10^{-6}$	$10{\cdot}10^{-6}$
Young's modulus [Pa]	$110{\cdot}10^{9}$	$22{\cdot}10^{9}$	$25{\cdot}10^{9}$
Poisson's ratio [−]	0.35	0.15	0.2

For the thermal simulation a boundary condition of heat flux

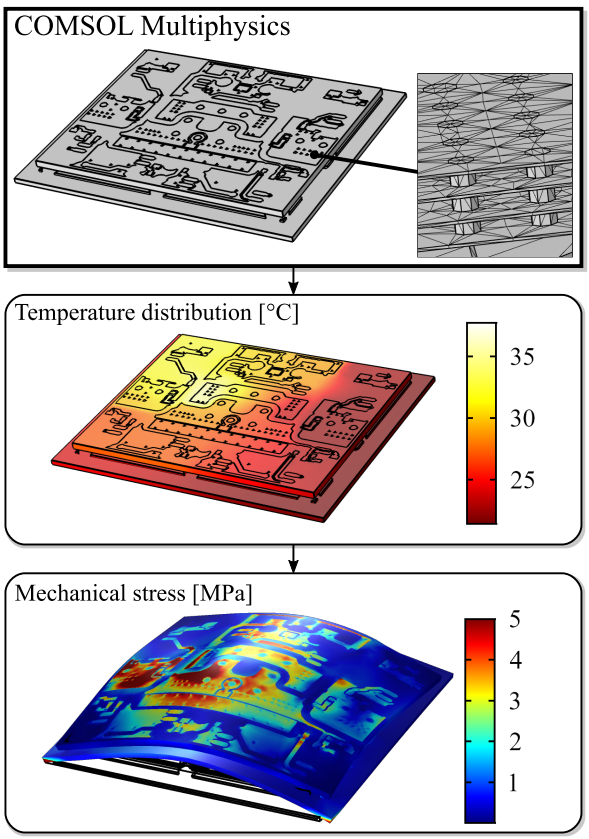

Fig. 3. COMSOL Multiphysics is used for the simulation, first solving the temperature distribution then using this to solve for thermo-mechanical induced stress/strain. The visualized deflection is multiplied by a factor 1000.

is assigned to the bottom surface of the DBC, as given by

$$q = h \cdot (T_{ext} - T) \tag{1}$$

where q is the heat flux, h is the heat transfer coefficient, T_{ext} the exterior temperature and T is the surface temperature, which is being solved for. The temperature distribution throughout the power module is greatly affected by how efficiently the power module can dissipate the heat given by (1), and thereby also impacts the amount of deflection. The heat transfer coefficient, h, may change by orders of magnitude depending on how the module is cooled. In literature, h is in the range of 100-300 $\frac{\mathrm{W}}{\mathrm{m^2\cdot K}}$ for modules cooled by forced convection, 500-2000 $\frac{\mathrm{W}}{\mathrm{m^2\cdot K}}$ for metal-to-metal contacts when modules are mounted to a heat sink and 10000 $\frac{\mathrm{W}}{\mathrm{m^2\cdot K}}$ or more for direct liquid cooling [1], [2], [33]–[35]. In a previous experimental study of this power module [7], the transient temperature response of the four GaN devices was monitored using fiber optic temperature sensors, while active power dissipation was exerted. The thermal simulation matched the experimental transient temperature response of all four devices when using a heat transfer coefficient, h = 1800 $\frac{W}{m^2K}$, which is within the common range of a power module mounted on a heat sink.

The deflection measurement method should be as least intrusive as possible, meaning that the drilled hole in the heat sink should not have significant impact on the thermal

performance. If the measurement method is intrusive and has too much impact on the system behavior, and the simulation model is adjusted for this change in system dynamics, it is no longer the in situ stress/strain in the real application that is being verified. This would limit the value offered by the digital replica, because it only resembles the test rig in the laboratory and not the module in its target application. The COMSOL Multiphysics model is used to evaluate the device temperatures when varying the diameter of a circle placed at the center of the DBC which is unable to dissipate heat. The simulation is done at a power input of 5 W to device Q_1, an ambient temperature of 20 °C and the hole diameter is varied from 0 to 20 mm. The results are shown in Fig. 4, and shows a 5 mm hole in the heat sink aligned with the center of the DBC has an impact of less than 1 % on any of the device temperatures. The steady state temperature distribution of the thermal simulation is used as the input to the next step of the simulation, as shown in Fig. 3, which is to include the thermomechanical effects due to the mismatch in CTE. For this simulation step it requires a new set of mechanical boundary conditions. The plastic housing, as shown in Fig. 2, is mounted with bolts in either end, and the plastic housing loads the perimeter of the DBC. The mechanical properties of the housing are not available and because of this, the housing is not included in the simulated 3D model. Instead, for this paper, idealized boundary conditions are assigned in COMSOL Multiphysics. The simulation is run with two sets of mechanical boundary conditions. In one case, as shown in Fig. 5(a), the plastic housing is regarded as completely rigid, meaning that it ensures that the entire perimeter of the DBC is fixed in the z-axis. The housing has some tolerance to the DBC, meaning that the DBC is free to expand in x and y-axes, as indicated by the arrows. In the simulation, one of the corners is fixed in both x, y and z-axes. Otherwise the model is free to move and rotate, because its orientation in space would not be fully defined. For an electrical equivalent, this is similar to defining the electric ground. Voltage differences between internal nodes do not change based on which node is defined as ground, but it provides a point of reference. In the other case, shown in Fig. 5(b), because that the housing is only fixed at two ends, it is regarded that the housing itself slightly bends. This means that the DBC is only fixed in the z-axis at the two ends where the bolts are located. Again, the same corner is used as mechanical point of reference, and the DBC is free to expand in x and y-axes as indicated by the arrows. In the remainder of the paper, the two sets of boundary conditions are denoted as simulation A and simulation B, respectively.

Because the experiment only measures the deflection at a single point, the tests are done at several power dissipation levels in the power module. This is to ensure that the deflection scales similarly in the simulation and the experiment, hence that they comply at several operating conditions. Tests are performed by applying a DC current of 5 A, 10 A and 12 A, which for 50 mΩ semiconductor drain-source resistance corresponds to a power dissipation of 1.25 W, 5 W and 7.2 W, respectively.

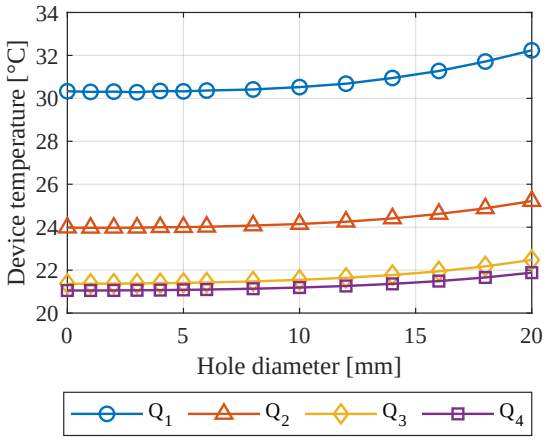

Fig. 4. Simulated device temperatures as a function of diameter of the hole drilled through the heatsink, with 5 W power dissipation in Q_1 and ambient temperature 20 °C.

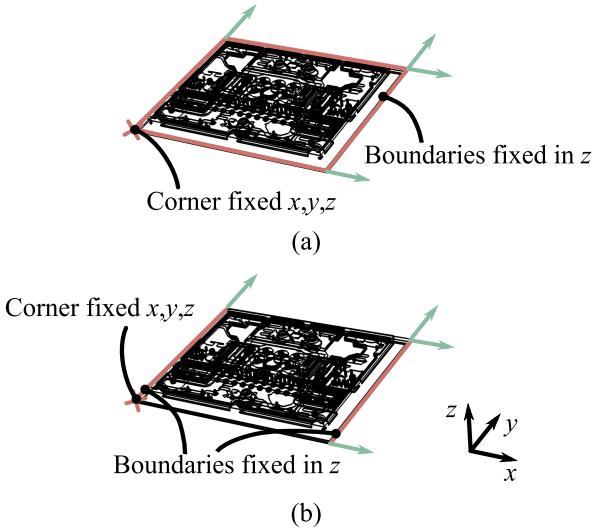

Fig. 5. Mechanical boundary conditions where (a) the frame is regarded rigid and entire boundary is fixed in z-axis and (b) only the two ends with bolts clamping are fixed in z-axis.

IV. Experimental Tests

The experimental setup is prepared as described in the following. Mounting the power module is done by applying a layer of thermal interface material in between the heat sink and the DBC. Metal clamps on the housing allows for fixating the power module to the heat sink. The top of the plastic housing is milled off for easier access with wires from a laboratory DC power supply to control the GaN eHEMT devices on/off. It also allows for connecting a high current DC power supply to drive a constant current through the drain-source of the device under test. This bypasses the original gate driver circuit, meaning that bootstrap gate driver circuitry shown on the PCB in Fig. 6 is omitted. A Ø4 mm hole is drilled to the heat sink, as this was found adequate to have the correct angle of incidence, and it is not intrusive to the thermal performance as indicated by Fig. 4. The Keyence LK-G3001 laser displace-

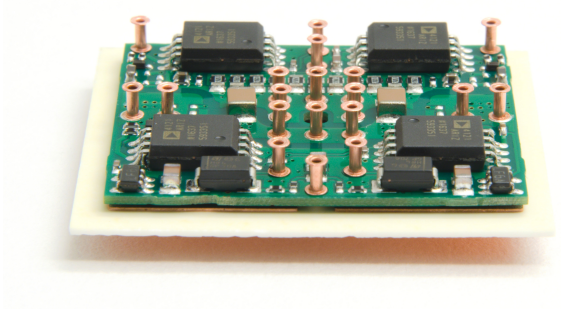

Fig. 6. Picture of the manufactured integrated GaN eHEMT power module without pins and housing.

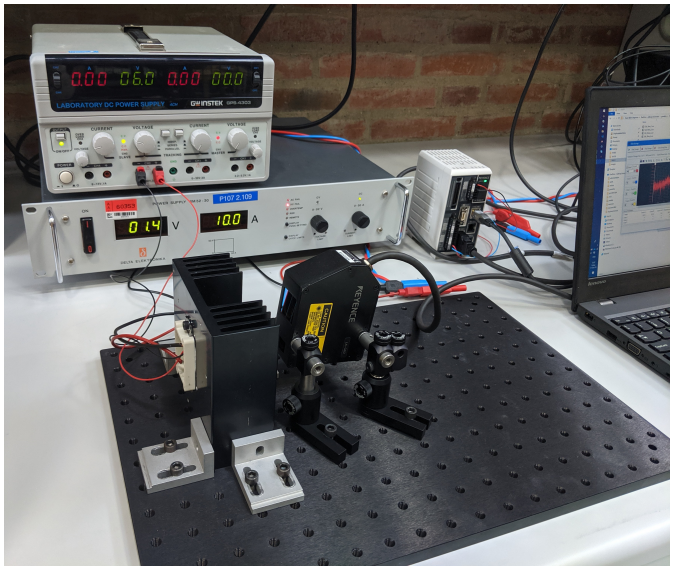

Fig. 7. Picture of the test setup, showing a laboratory DC-supply for the gate-source control, high power DC-supply for drain-source current, the power module mounted on a heat sink, the Keyence laser displacement sensor and its controller for datalogging.

ment sensor is mounted and aligned to point through the hole, as shown in Fig. 7. The heatsink and the laser displacement sensor are both mounted on a solid aluminium base to ensure alignment throughout the experiment. A Keyence LK-G5001 controller is used for datalogging and enables control of the laser displacement sensor from a PC through USB-interface.

A. Initial evaluation of setup

In this section the initial drift of the displacement measurement and the measurement inaccuracy is investigated. The Keyence laser displacement sensor might have some internal dynamics which are studied before the tests are done. The electronic circuitry in the sensor has a temperature dependency. Initially when the laser starts up, it will experience some drift until the internals are heated up to a steady state temperature. The test is done in the following manner. As the sensor is powered up, it connects to the PC and data logging is initialized. The logging starts as soon as possible, but as it is a manual task to operate the graphical user interface, it takes around 10 seconds or less to run after power up. The measured displacement of the laser displacement sensor is logged on four

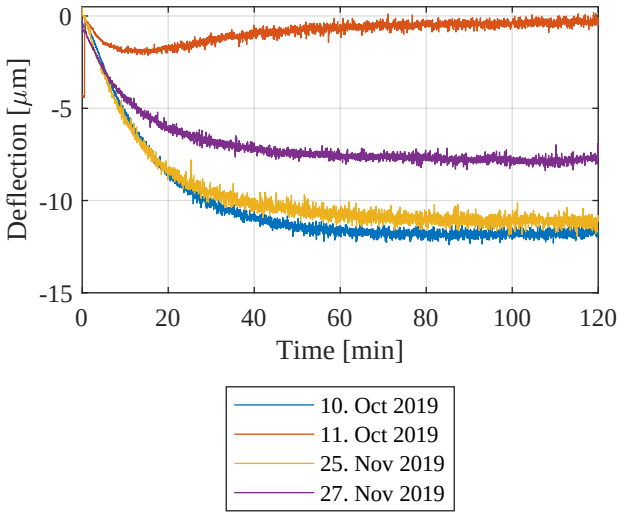

Fig. 8. Drift in the measurements of the laser displacement sensor just after start up.

different days from a "cold" startup, and the results are shown in Fig. 8. There is no power dissipated in the power module, thus the measured deflection is only due to the drift in the measurements of the laser displacement sensor itself. After roughly 80-100 minutes the deflection has reached a steady state level. Based on this result, in this paper a minimum of 100 minutes has been used to heat up the laser displacement sensor to avoid influence of thermal drift of the sensor itself.

After the initial drift of the sensor has settled, a measurement of the displacement during three minutes is done. This is done to investigate the inaccuracy of the sensor. Once again, there is no voltage applied and thereby no power dissipated anywhere in the power module. The results are shown in Fig. 9, which both shows the logged measurement points during time and shown as a histogram in intervals of 0.05 μm per bar. Assuming that the inaccuracy of measurement data is random and follows a normal distribution, the mean is zero and a standard deviation of 0.133 μm, as plotted in the solid line of the histogram of Fig. 9.

B. Deflection measurements

Following the initial investigation of the measurement system, deflection measurement tests are performed at three different DC current levels of 5 A, 10 A and 12 A, which for the 50 mΩ on-resistance of the device corresponds to a power loss of 1.25, 5 and 7.2 W, respectively. The power loss is sustained for 10 minutes to ensure that the power module and the heat sink has reached a thermal equilibrium. Because of the deflections being in a range of only a few μm, and because of the inaccuracy of the deflection measurement itself, four tests are performed at each current level. The obtained results are shown in Fig. 10, where each color corresponds an individual test run and the solid black line is the average of all four. The dashed line is the final steady state value achieved in the test.

The results of Table II show that the lowest error between simulation and experiment is obtained for the case of using

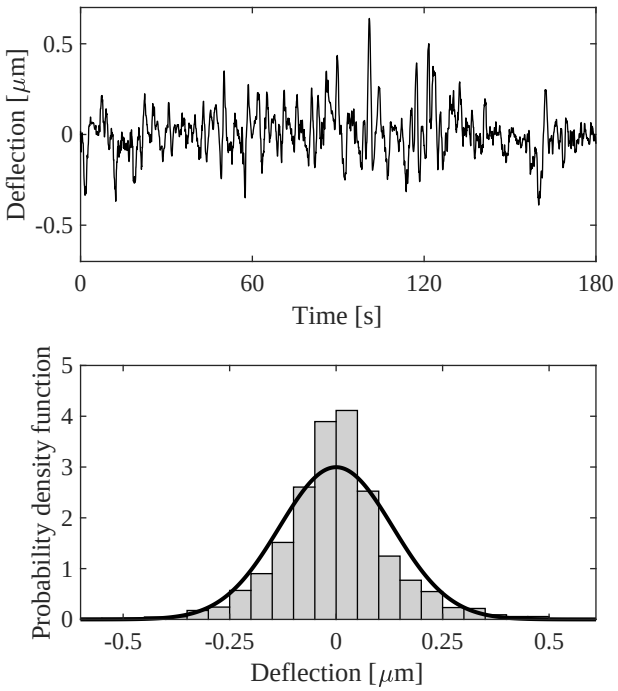

Fig. 9. Measurements during 180 seconds with sampling period 4 ms (top), and its associated histogram and probability density function (bottom).

TABLE II
COMPARISON OF SIMULATED AND MEASURED DEFLECTIONS

	1.25 W	**5 W**	**7.2 W**
Simulation constraint A	0.35 μm	1.41 μm	2.03 μm
Simulation constraint B	0.60 μm	2.41 μm	3.63 μm
Experiment	0.61 μm	2.49 μm	3.38 μm
Error: Sim_A - Exp	-42.6 %	-43.4 %	-39.9 %
Error: Sim_B - Exp	-1.6 %	-3.2 %	7.3 %

constraint B. It is concluded that the simulation results obtained using constraint A are not valid. This assumed the plastic housing to be a rigid frame, limiting any movement of the DBC perimeter in the z-direction. The simulation with constraint B is the case where the power module is fixed in the z-axis only at the two edges that are close to the bolts of the housing, as previously shown in Fig. 5. For the simulation with constraint B the maximum observed relative error is 7.3 %, corresponding to an absolute error of 0.25 μm. Furthermore, it is observed that the deflection in the experiment scales linearly with the input power loss, which indicates that the stress/strain relationship is within the elastic linear region of the materials. It is concluded that there is a good correspondence with the experimental results, and thus that the simulation with constraint B is a valid model to predict the thermomechanical stress of the module.

V. DISCUSSION & FUTURE WORK

The methodology proposed in this paper requires visible access to the DBC or baseplate of the device under test. Furthermore, the laser displacement sensor used requires a

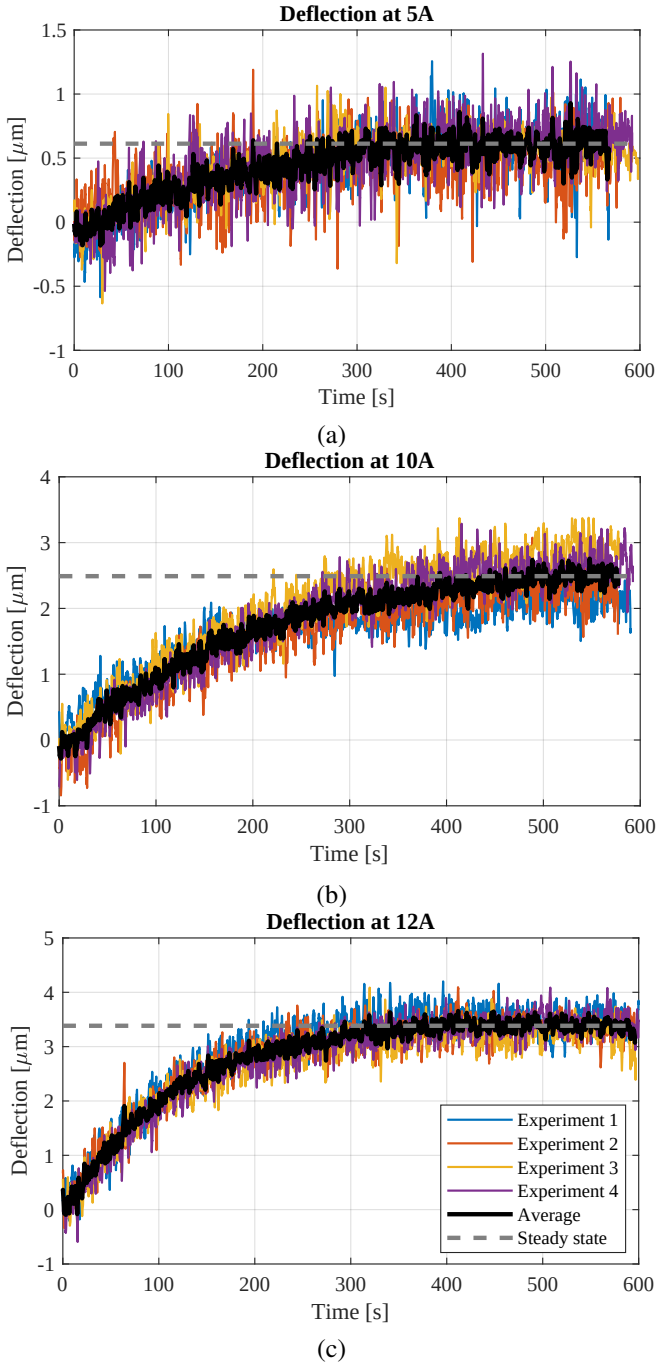

Fig. 10. Deflection measured of power module at current levels of (a) 5 A (b) 10 A and (c) 12 A.

slight angle of incidence to operate. This means that the method might not be applicable for use with power modules cooled by direct liquid cooling, or if the heat sink has obstacles blocking the angle of incidence, such as a large number of pin fins. In the latter case, a Michelson interferometer configuration is deemed a viable solution as the beam is normal to the measured surface.

Once the simulation model has been verified, it has the potential to investigate and understand several stress mechanisms of the power module, each responsible for specific

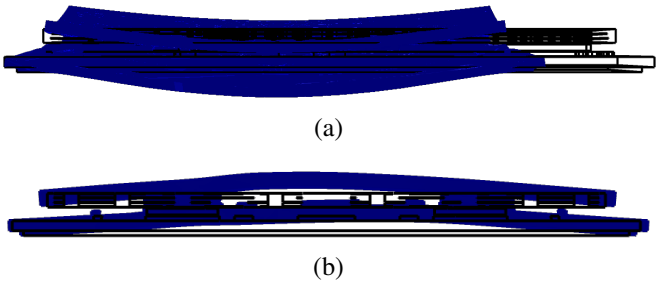

(a)

(b)

Fig. 11. Cross-sectional view of deformation (scaled 250 times) during (a) uniform temperature at -25 degree celsius, compared to reference of 20 degree celsius and (b) active heating of 12 A.

failure modes [10]. Designing an experimental test rig to target a specific failure mode or loading profile is often difficult and time consuming [36]–[38]. The time until failure is often several weeks long, and the module is tested at several stressor levels to map its influence on the lifetime [39]. With the improvement in simulation software packages and the increase in computing power, it increases the viability of using the software tools to assess individual failure modes and reliability issues of power module packages [19]–[21].

The following paragraph discusses the difference between a passive thermal and active heat up of the power module, using the verified simulation model to simulate both cases. The former refers to the case where a power module is placed in a thermal chamber, and the temperature is ramped up, often in a large temperature range i.e. -25 to 125 degree celsius to quickly cause fatigue during a few hundred cycles. The latter is, when the temperature increase of the power module is caused by a power loss dissipated in one of the semiconductor devices, similar to the experiment used in this paper. For passive thermal cycling, as the temperature is cycled both to negative and positive temperatures compared to the reference temperature of 20 degree celsius, it experiences both convex and concave bending of the DBC. The deflection at -25 degree celsius is shown in Fig. 11(a). In the active heating, a power step input is given to one of the devices in the power module, where the generated heat is conducted through the DBC and to the heat sink. Because the top side copper has a higher temperature than the bottom side copper it will expand more. Thus, the bend in this case is always concave compared to the reference, as shown in Fig. 11(b). This example serves the purpose of highlighting how the "passive" and "active" temperature profiles cause differences in stress and thereby potentially highlights different failure modes. During the lifetime of a power module it will experience both types of stress, including many other scenarios that are increasingly difficult to build a specific test rig for each case. The simulation is a viable tool to rapidly visualize the potential locations of stress in the power module caused by several operation conditions. This offers, during the early digital design phase, the ability to ensure that stress-strain characteristics stay within known material robustness margins, to allow a high performance design even prior to prototyping and physical testing.

At present it is not certain how effective the FEM software and digital tools are to predict long-term degradations, such as those occurring on a scale smaller than a typical mesh-size [21]. Such failure mechanisms could be degradation of metallization surfaces [40], crack propagations dependent on micron-size grains [41] and mass diffusion caused by current cycling in solder joints [42]. The common obstacle to predict such failure mechanisms using software, are that they occur on a small size and long time-scale, which results in an overflow of memory and unpractical computational time. Future work is focused on determining the accuracy of the digital tools to predict the locations of failure in the power module.

VI. Conclusion

This paper has presented a FEM simulation of the thermo-mechanical induced stress/strain of an integrated GaN power module. To verify the simulation model and its boundary conditions, an experimental test is used to verify the deflection of the DBC of the power module. In literature commonly the power module is removed from its intended application. In this paper, a method is proposed using a laser displacement sensor to measure the deflection in a single point of the power module during operation. The experiment is performed at DC power levels of 1.25 W, 5 W and 7.2 W dissipated in one of the GaN semiconductor devices of the module, and the deflection during time is monitored. The steady state results are compared with the FEM simulation. For one set of boundary conditions the maximum absolute error is 0.25 μm. This was measured at the maximum observed deflection of 3.38 μm, thus corresponds to 7.3 % error. It is concluded that the proposed method is a valuable tool to identify proper FEM simulation models that will allow accurate stress/strain predictions. Future research is focused on studying the stress/strain distribution of the power module in detail and predict the points with highest risk of mechanical failure, as the power module is subjected to lifetime wear out tests.

References

[1] G. Feix, E. Hoene, O. Zeiter, and K. Pedersen, "Embedded Very Fast Switching Module for SiC Power MOSFETs," in *Proceedings of PCIM Europe 2015; International Exhibition and Conference for Power Electronics, Intelligent Motion, Renewable Energy and Energy Management*, Nuremberg, Germany, 2015, pp. 1–7.

[2] D. Kearney, S. Kicin, E. Bianda, A. Krivda, D. Bauman, and A. B. B. Corporate, "PCB Embedded Power Electronics for Low Voltage Applications," in *CIPS 2016 - 9th International Conference on Integrated Power Electronics Systems*, 2016, pp. 3–8.

[3] K. Klein, E. Hoene, R. Reiner, and R. Quay, "Study on Packaging and Driver Integration with GaN Switches for Fast Switching," in *CIPS 2016; 9th International Conference on Integrated Power Electronics Systems*, March 2016, pp. 1–6.

[4] A. B. Jørgensen, S. Bęczkowski, C. Uhrenfeldt, N. H. Petersen, S. Jørgensen, and S. Munk-Nielsen, "A Fast-Switching Integrated Full-Bridge Power Module Based on GaN eHEMT Devices," *IEEE Transactions on Power Electronics*, vol. 34, no. 3, pp. 2494–2504, 2019.

[5] A. E. Risseh, H. Nee, and K. Kostov, "Fast Switching Planar Power Module With SiC MOSFETs and Ultra-low Parasitic Inductance," in *2018 International Power Electronics Conference (IPEC-Niigata 2018 -ECCE Asia)*, 2018, pp. 2732–2737.

[6] Y. Ren, X. Yang, F. Zhang, L. Tan, and X. Zeng, "Analysis of a Low-Inductance Packaging Layout for Full-SiC Power Module Embedding Split Damping," in *2016 IEEE Applied Power Electronics Conference and Exposition (APEC)*, 2016, pp. 2102–2107.

[7] A. B. Jørgensen, T. Cheng, D. Hopkins, S. Beczkowski, C. Uhrenfeldt, and S. Munk-Nielsen, "Thermal Characteristics and Simulation of an Integrated GaN eHEMT Power Module," in *2019 21st European Conference on Power Electronics and Applications (EPE '19 ECCE Europe)*, Sep. 2019, pp. P.1–P.7.

[8] C. Yu, . Labouré, and C. Buttay, "Thermal Management of Lateral GaN Power Devices," in *2015 IEEE International Workshop on Integrated Power Packaging (IWIPP)*, 2015, pp. 40–43.

[9] A. B. Jørgensen, S. Munk-Nielsen, and C. Uhrenfeldt, "Overview of Digital Design and Finite Element Analysis in Modern Power Electronic Packaging," *IEEE Transactions on Power Electronics*, pp. 1–1, 2020.

[10] Y. Xu, Z. Xu, J. W. Eischen, and D. C. Hopkins, "FEA-Based Thermal-Mechanical Design Optimization for DBC Based Power Modules," in *IEEE International Symposium on 3D Power Electronics Integration and Manufacturing (3D-PEIM)*, 2016, pp. 1–6.

[11] L. Xu, M. Wang, Y. Zhou, Z. Qian, and S. Liu, "An Optimal Structural Design to Improve the Reliability of Al2O3–DBC Substrates under Thermal Cycling," *Microelectronics Reliability*, vol. 56, pp. 101 – 108, 2016.

[12] N. Heuck, R. Bayerer, S. Krasel, F. Otto, R. Speckels, and K. Guth, "Lifetime Analysis of Power Modules with New Packaging Technologies," in *2015 IEEE 27th International Symposium on Power Semiconductor Devices IC's (ISPSD)*, 2015, pp. 321–324.

[13] R. Nielsen, J. Due, and S. Munk-Nielsen, "Innovative Measuring System for Wear-out Indication of High Power IGBT Modules," in *2011 IEEE Energy Conversion Congress and Exposition*, 2011, pp. 1785–1790.

[14] U. Choi, F. Blaabjerg, and S. Jørgensen, "Power Cycling Test Methods for Reliability Assessment of Power Device Modules in Respect to Temperature Stress," *IEEE Transactions on Power Electronics*, vol. 33, no. 3, pp. 2531–2551, 2018.

[15] M. Held, P. Jacob, G. Nicoletti, P. Scacco, and M. . Poech, "Fast Power Cycling Test of IGBT modules in Traction Application," in *Proceedings of Second International Conference on Power Electronics and Drive Systems*, vol. 1, 1997, pp. 425–430 vol.1.

[16] H. Berg and E. Wolfgang, "Advanced IGBT modules for railway traction applications: Reliability testing," *Microelectronics Reliability*, vol. 38, no. 6, pp. 1319 – 1323, 1998, reliability of Electron Devices, Failure Physics and Analysis.

[17] C. Durand, M. Klingler, D. Coutellier, and H. Naceur, "Power Cycling Reliability of Power Module: A Survey," *IEEE Transactions on Device and Materials Reliability*, vol. 16, no. 1, pp. 80–97, 2016.

[18] K. Ma, H. Wang, and F. Blaabjerg, "New Approaches to Reliability Assessment: Using Physics-of-Failure for Prediction and Design in Power Electronics Systems," *IEEE Power Electronics Magazine*, vol. 3, no. 4, pp. 28–41, Dec 2016.

[19] Y. Jia, Y. Huang, F. Xiao, H. Deng, Y. Duan, and F. Iannuzzo, "Impact of Solder Degradation on VCE of IGBT Module: Experiments and Modeling," *IEEE Journal of Emerging and Selected Topics in Power Electronics*, pp. 1–1, 2019.

[20] L. Yang, P. A. Agyakwa, and C. M. Johnson, "Physics-of-Failure Lifetime Prediction Models for Wire Bond Interconnects in Power Electronic Modules," *IEEE Transactions on Device and Materials Reliability*, vol. 13, no. 1, pp. 9–17, March 2013.

[21] O. Dalverny and J. Alexis, "Thermo-mechanical Behavior of Power Electronic Packaging Assemblies: From Characterization to Predictive Simulation of Lifetimes," *AIP Conference Proceedings*, vol. 1932, no. 1, p. 030009, 2018.

[22] M.-C. Liao, P.-S. Huang, Y.-H. Lin, M.-Y. Tsai, C.-Y. Huang, and T.-C. Huang, "Measurements of Thermally-Induced Curvatures and Warpages of Printed Circuit Board during a Solder Reflow Process Using Strain Gauges," *Applied Sciences*, vol. 7, no. 7, 2017.

[23] G. Mirone, A. Sitta, G. D'Arrigo, and M. Calabretta, "Material Characterization and Warpage Modeling for Power Devices Active Metal Brazed Substrates," *IEEE Transactions on Device and Materials Reliability*, vol. 19, no. 3, pp. 537–542, Sep. 2019.

[24] C. Uhrenfeldt, S. Munk-Nielsen, and S. Bęczkowski, "Frequency Domain Scanning Acoustic Microscopy for Power Electronics: Physics-based Feature Identification and Selectivity," *Microelectronics Reliability*, vol. 88-90, pp. 726 – 732, 2018, 29th European Symposium on Reliability of Electron Devices, Failure Physics and Analysis (ESREF 2018).

[25] F. Naumann, G. Lorenz, M. Bernasch, B. Boettge, C. Ebensperger, and S. Oehling, "Thermo-mechanical Stress and Deformation Behavior of Joined Semiconductor Devices using Different Die Attach Technologies," in *CIPS 2018; 10th International Conference on Integrated Power Electronics Systems*, March 2018, pp. 1–6.

[26] J. Sommer, R. Bayerer, R. Tschirbs, and B. Michel, "Base Plate Shape Optimisation for High-Power IGBT Modules," in *5th International Conference on Integrated Power Electronics Systems*, March 2008, pp. 1–4.

[27] C. Zhang, Y. Kim, and L. Xu, "A Study on Novel Integrated Base Plate (IBP) Package for Power Electronics Module," in *2019 IEEE International Conference on Electron Devices and Solid-State Circuits (EDSSC)*, June 2019, pp. 1–3.

[28] Y. Liu, Y. Liu, Z. Yuan, T. Chen, K. Lee, and S. Belani, "Warpage Analysis and Improvement for a Power Module," in *2013 IEEE 63rd Electronic Components and Technology Conference*, May 2013, pp. 475–480.

[29] GaN Systems Inc, "Top-side cooled 650 V E-mode GaN transistor," Accessed: 2020-05-27. [Online]. Available: https://eu.mouser.com/datasheet/2/692/GS66508T-DS-Rev-180213-1314197.pdf

[30] K. Azar and J. E. Graebner, "Experimental Determination of Thermal Conductivity of Printed Wiring Boards," in *Twelfth Annual IEEE Semiconductor Thermal Measurement and Management Symposium. Proceedings*, March 1996, pp. 169–182.

[31] F. Sarvar, N. J. Poole, and P. A. Witting, "PCB Glass-Fibre Laminates: Thermal Conductivity Measurements and Their Effect on Simulation," *Journal of Electronic Materials*, vol. 19, no. 12, pp. 1345–1350, Dec 1990.

[32] W. W. Sheng and R. P. Colino, *Power Electronic Modules Design and Manufacture*. Boca Raton, Florida: CRC Press LLC, 2005.

[33] C. Qian, A. M. Gheitaghy, J. Fan, H. Tang, B. Sun, H. Ye, and G. Zhang, "Thermal Management on IGBT Power Electronic Devices and Modules," *IEEE Access*, vol. 6, pp. 12 868–12 884, 2018.

[34] I. Mudawar, D. Bharathan, K. Kelly, and S. Narumanchi, "Two-Phase Spray Cooling of Hybrid Vehicle Electronics," *IEEE Transactions on Components and Packaging Technologies*, vol. 32, no. 2, pp. 501–512, June 2009.

[35] R. Skuriat and C. M. Johnson, "Direct Substrate Cooling of Power Electronics," in *5th International Conference on Integrated Power Electronics Systems*, March 2008, pp. 1–5.

[36] V. Smet, F. Forest, J. Huselstein, F. Richardeau, Z. Khatir, S. Lefebvre, and M. Berkani, "Ageing and Failure Modes of IGBT Modules in High-Temperature Power Cycling," *IEEE Transactions on Industrial Electronics*, vol. 58, no. 10, pp. 4931–4941, Oct 2011.

[37] R. Schmidt and U. Scheuermann, "Separating Failure Modes in Power Cycling Tests," in *2012 7th International Conference on Integrated Power Electronics Systems (CIPS)*, March 2012, pp. 1–6.

[38] R. Bayerer, T. Herrmann, T. Licht, J. Lutz, and M. Feller, "Model for Power Cycling lifetime of IGBT Modules - Various Factors Influencing Lifetime," in *5th International Conference on Integrated Power Electronics Systems*, March 2008, pp. 1–6.

[39] L. Ceccarelli, R. M. Kotecha, A. S. Bahman, F. Iannuzzo, and H. A. Mantooth, "Mission-Profile-Based Lifetime Prediction for a SiC MOSFET Power Module Using a Multi-Step Condition-Mapping Simulation Strategy," *IEEE Transactions on Power Electronics*, vol. 34, no. 10, pp. 9698–9708, Oct 2019.

[40] M. Brincker, K. Bonderup Pedersen, P. K. Kristensen, and V. Popok, "Passive Thermal Cycling of Power Diodes under Controlled Atmospheric Conditions - Effects on Metallization Degradation," in *CIPS 2016; 9th International Conference on Integrated Power Electronics Systems*, March 2016, pp. 1–6.

[41] K. B. Pedersen, P. K. Kristensen, V. Popok, and K. Pedersen, "Degradation Assessment in IGBT Modules Using Four-Point Probing Approach," *IEEE Transactions on Power Electronics*, vol. 30, no. 5, pp. 2405–2412, May 2015.

[42] H. Ye, C. Basaran, and D. C. Hopkins, "Mechanical Degradation of Microelectronics Solder Joints under Current Stressing," *International Journal of Solids and Structures*, vol. 40, no. 26, pp. 7269 – 7284, 2003.

Asger Bjørn Jørgensen received the M.Sc. degree in energy engineering with a specialization in power electronics and the Ph.D. degree from Aalborg University, Aalborg, Denmark, in 2016 and 2019, respectively.

He is currently working as a Postdoctoral with the Department of Energy Technology, Aalborg University. His research interests include power module packaging, wide bandgap power semiconductors and multiphysics finite-element analysis.

Stig Munk-Nielsen received the M.Sc. and Ph.D. degrees in electrical engineering from Aalborg University, Aalborg, Denmark, in 1991 and 1997, respectively.

He is currently working as a Professor WSR with the Department of Energy Technology, Aalborg University. He has been involved or has managed 12 research projects, including both national and European Commission projects. His research interests include low- and medium-voltage converters, packaging of power electronic devices, wide bandgap semiconductors, electrical monitoring apparatus for devices, failure modes, and device test systems.

Christian Uhrenfeldt received the M.Sc. degree in physics from Aalborg University, Aalborg, Denmark, in 2004, and the Ph.D. degree in the field of semiconductor material science from Aarhus University, Aarhus, Denmark, in 2008.

He is currently working as an Associate Professor with the Department of Energy Technology, Aalborg University, on power electronics packaging and materials. His research interests include packaging of power modules, nondestructive testing and semiconductor diagnostics in power electronics.